Study of Resolution for Harmonic Drives Controller with Friction in Precision Robotic System

Shao-wen Le, Gang-jun Li
Electromechanical engineering Department,
Chengdu ElectroMechanical College
Chengdu, China

***Abstract*—The friction model with the effects of friction and transmission flexibility of harmonic drives system is used for resolution study in precision control system. First, the resolution of a linear controller and an impulse controller in robotic manipulator system are studied respectively, then friction effect on resolution of impulse control system is investigated. Simulation and experiments show that the resolution of impulse control is much better than that of linear control, the friction in harmonic drive degrades the performance of impulse control, this will benefit the use of harmonic drive in precision control system.**

Keywords- resolution; controller; harmonic drives; precision systems

I. INTRODUCTION

Harmonic drive has captured more and more researcher's attention in the last decades. Because it has many advantages including near-zero backlash, high gear reduction ratio and compact design, and A number of researchers have devised impulse controllers that can achieve precise positioning in the presence of friction[1][2][3][4], it is more and more widely used in precision robotic control systems. For example, in the optoelectronic automation industry, the process of attaching optical fibres to optoelectronic devices requires submicron alignment accuracy in positioning. However, the nonlinear attributes of friction and flexibility in harmonic drives are responsible for performance degradation.

One of the most critical performance characteristics of the precision robotic manipulator is the ability to consistently move in small motion increments. This characteristic is known as resolution and is defined as the smallest reproducible motion step that the robotic system can consistently make during point to point motion. A system's resolution effectively puts an upper limit on the repeatability and precision that can be achieved even with closed-loop feedback. The resolution of a system should be verified experimentally since it often depends on subtle system dynamic factors that are difficult to model; these can include gear meshing, bearing noise, and transmission stiffness. Statistical measurements should also be used since the factors that influence resolution can vary over time and the range of the mechanism.

The resolutions of one mechanism for different inputs may be different. For example, the resolution for a linear controller is different from that for an impulse controller. The resolutions under these two controllers are tested as follows.

II. NON-DIMENSIONAL EQUATION OF FRICTION MODEL

A harmonic drive in precision robotic control system can be modelled as two masses connected with a spring, as shown in Fig.1. The control input acts on the motor and wave-generator inertia J_m, which is connected via a gear reduction r to the flexspline and arm inertia J_l. The flexibility of the harmonic drive motor plays a significant role in system dynamics and is modelled using a torsional spring that produces a torque T_s.

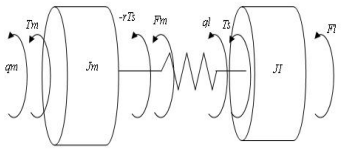

Fig. 1. Harmonic drive model

F_m and F_l stand for frictions in motor side and load side respectively, q_m and q_l are the positions of motor and load. The system's mathematical model can stated as[5]:

$$J_m\ddot{q}_m = -F_m - rK_s(r\ddot{q}_m - q_l) - \frac{K_m K_b}{R}\dot{q}_m + \frac{K_m}{R}u(t) \quad (1)$$

$$J_l\ddot{q}_l = -F_l + K_s(rq_m - q_l) \quad (2)$$

where K_s is a spring constant of the harmonic drive, K_m is the motor torque constant; $u(t)$is the input voltage, R is armature resistance, K_b is voltage constant.

when the velocity is not zero and we neglect the viscous friction, set $f_m = f_{sm} = f_{cm}$, $f_l = f_{sl} = f_{cl}$, f_{sm} and f_{cm} are motor side static friction and Coulomb friction. f_{sl} And f_{cl} are load side static friction and Coulomb friction, the friction can be written as:

$$F_m = -\mathrm{sgn}(\dot{q}_m)f_m \quad (3)$$

$$F_l = -\mathrm{sgn}(\dot{q}_l)f_l \quad (4)$$

The motor input torque is $T_m = -\frac{K_m K_b}{R}\dot{q}_m + \frac{K_m}{R}u(t)$, then equation (1) and (2) can be written as:

$$J_m\ddot{q}_m = -\mathrm{sgn}(\dot{q}_m)f_m - rK_s(rq_m - q_l) + T_m \quad (5)$$

$$J_l\ddot{q}_l = -\mathrm{sgn}(\dot{q}_l)f_l + K_s(rq_m - q_l) \quad (6)$$

This work was supported by Sichuan Natural Science foundation under Grant No.2010GZ0127

We define system characteristic frequency as:

$$\omega_m = \sqrt{\frac{f_m}{J_m}} \tag{7}$$

then the system characteristic time is:

$$T_c = \frac{1}{\omega_m} = \sqrt{\frac{J_m}{f_m}} \tag{8}$$

The non-dimensional time is defined as:

$$t^* = \frac{t}{T_c} \tag{9}$$

Then

$$t = T_c t^* \tag{10}$$

$$dt = T_c dt^* \tag{11}$$

(5) and (6) can be written as:

$$\frac{d^2 q_m}{(dt^*)^2} = -\frac{T_c^2 f_m}{J_m}\operatorname{sgn}(\frac{dq_m}{dt^*}) - \frac{T_c^2 r K_s}{J_m}(rq_m - q_l) + \frac{T_c^2 T_m}{J_m}$$
$$= -\operatorname{sgn}(\frac{dq_m}{dt^*}) - \frac{rK_s}{f_m}(rq_m - q_l) + \frac{T_m}{f_m} \tag{12}$$

$$\frac{d^2 q_l}{(dt^*)^2} = -\frac{T_c^2 f_l}{J_l}\operatorname{sgn}(\frac{dq_l}{dt^*}) - \frac{T_c^2 r K_s}{J_l}(rq_m - q_l)$$
$$= -\frac{J_m f_l}{J_l f_m}\operatorname{sgn}(\frac{dq_l}{dt^*}) + \frac{J_m K_s}{J_l f_m}(rq_m - q_l) \tag{13}$$

In order to understand how the parameter variations affect the output displacement and make the following analysis more general to other systems, we define following non-dimensional parameters:

$$K^* = \frac{K_s}{f_m} \tag{14}$$

$$J_l^* = \frac{J_l}{J_m} \tag{15}$$

$$f_l^* = \frac{f_l}{f_m} \tag{16}$$

$$\tau^* = \frac{T_m}{f_m} \tag{17}$$

$$r^* = r \tag{18}$$

The substitution of (14) to (18) in equations (12) and (13) yields:

$$\frac{d^2 q_m}{(dt^*)^2} = -\operatorname{sgn}(\frac{dq_m}{dt^*}) - r^* K_s^* (r^* q_m - q_l) + \tau^* \tag{19}$$

$$\frac{d^2 q_l}{(dt^*)^2} = -\frac{f_l^*}{J_l^*}\operatorname{sgn}(\frac{dq_l}{dt^*}) + \frac{K_s^*}{J_l^*}(r^* q_m - q_l) \tag{20}$$

III. Resolution for Linear Controller with Motor Position Feedback

In order to study the resolution of harmonic drive in precision robotic control systems, we built an exprimental apparatus. A robotic manipulator with three degrees of freedoms has two arms driven by harmonic drive motors and one linear stage actuated by a timing belt driven lead screw was previously developed. The manipulator is controled by a computer with an amplifier and an interface card. The interface card includes A/D, D/A and an encoder accessing device. Two capacitance sensors used to measure the position of the arms are parallel to the arms of the manipulator. The overall control scheme is illustrated in Fig.2.

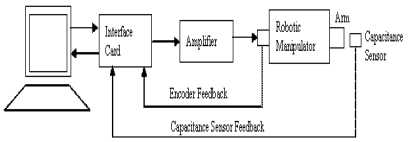

Fig. 2. Overall control scheme

For the linear controller we consider only the motor encoder sensor for feedback since it is the most common type used in industry. It is also much more practical (in terms of range) and more economical than other high accuracy sensors. The resolution test for the arm consists of 1000 steps in one direction from which a histogram of the resultant displacement is made. The displacements are determined using a capacitance sensor that measures the output of the arm. The initial step size used is one motor encode count. If this size produces inconsistent increments, the magnitude of the step is increased by one encoder count and the test is run again. This process is repeated until consistent motion is observed. The minimum value of the arm consistent increments is the resolution of the mechanism.

For the 1000 steps of one encoder count increment (approximately 1.5 um of arm displacement), the arm displacement is shown in Fig.3. The histogram of the arm displacement is shown in Fig.4.

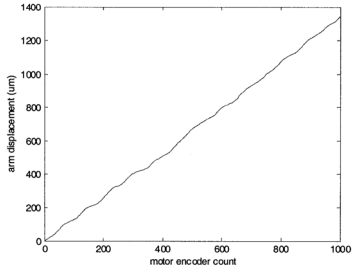

Fig.3 Arm displacements for 1000 encoder count steps

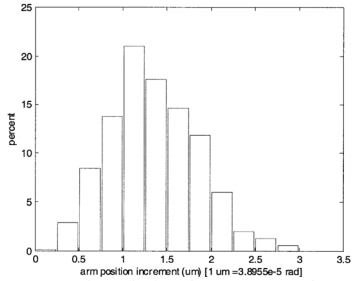

Fig.4 Histogram of resolution for 1000 encoder count steps

It is apparent from the histogram that consistent motion of one encoder count is possible. It should be noted that due to the non-Cartesian nature of the arm kinematics, one encoder count can represent between 1 um to 2um depending on the position of the sensor mounted. However, for most of the workspace, one encoder count is less than 1.5um; all motions that occur are less two encoder counts (3um). Therefore, the resolution of the arm for linear controller is 3um.

IV. RESOLUTION FOR IMPULSE CONTROLLER

For the resolution of the impulse controller, if the capacitance sensor is used for feedback, the motor can have a step motion less than one encoder count. To determine the resolution under impulse control, the pulse width is set to some nominal value (W=l ms) and the impulse amplitude is increased from zero until the smallest consistent arm motion is observed.

In order to obtain consistent resolution measurements from simulations and experiments, the following mathematical definition of resolution was used: A sequence of N impulse inputs with the same amplitude is applied to the system and the median and maximum value of the N increments is recorded. Starting from an impulse amplitude of zero, it is gradually increased until a consistent median increment is achieved that is larger than a small threshold tolerance ε_1. This threshold input is then multiplied by $(1+\varepsilon_2)$ where ε_2 is the small tolerance that provides consistent motion in the presence of small input and parameter variations. The maximum increment due to this input is defined as the resolution of the system.

In our application we set ε_1 =0.1um and ε_2 =0.01. This above definition was used to test the resolution under an impulse control with N=1000 pulses. The measured arm position is shown in Fig.5. The histogram of the arm increment is shown in Fig.6. It is evident from the histogram that almost all motion increments are less than 0.3um, so the resolution under impulse control is 0.30um.

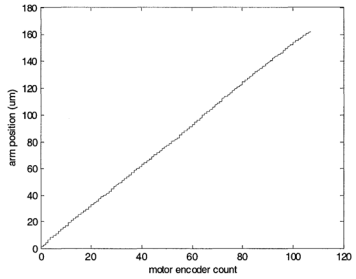

Fig.5 Arm displacements for 1000 impulse steps

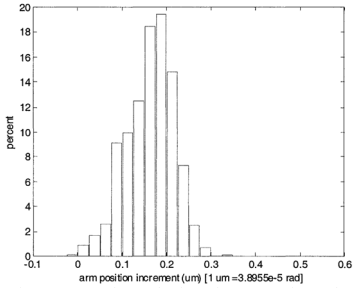

Fig.6 Histogram of resolution for 1000 impulse steps

V. FRICTION EFFECT ON RESOLUTION

The system parameters have a great effect on the impulse control effect such as resolution. We investigate friction effect on resolution by simulation and experiment as follows.

The load side friction level is f_l^* defined in equation (16). Take 25 friction levels from 0.01 to 1. For different friction levels, we use 1000 pulse inputs to simulate the resolution as defined above. A simulated histogram can be obtained. For example, the histograms for f_l^* =0.1 is plotted in Fig.7.

The simulation demonstrates that when friction level is big, the arm can only move after a number of pulses are applied and the spring deformation has accumulated to a certain amount. This is because the spring potential energy must accumulate to a certain amount to overcome the friction. The higher the friction level, the bigger the potential energy needed to drive the arm's motion. The first step of the delta is very big, and then gets smooth afterwards, as shown in Fig.8. The potential energy is accumulated before the load starts moving. Once the load moves, the system's potential energy decreases just like an avalanche.

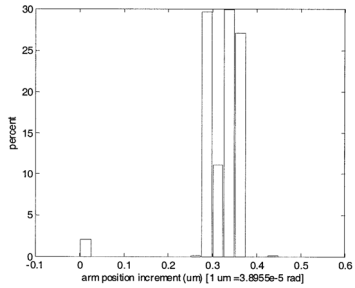

Fig.7 Simulation histogram for friction level f_l* =0.1 (1000 pulses)

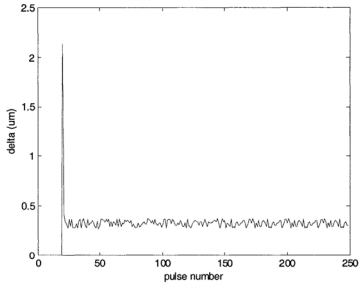

Fig.8 Delta versus pulse number, f_l* =0.1

For different friction levels, the maximum delta, median delta, and minimum delta are plotted in Fig.9 which shows that the resolution gets worse proportional to the friction level. We use the following equation to ca1culate the standard deviation:

$$\sigma = \sqrt{\frac{\sum_{i=1}^{N}(\delta_{average} - \delta_1)}{N-1}}$$

The standard deviation is plotted in Fig.10.

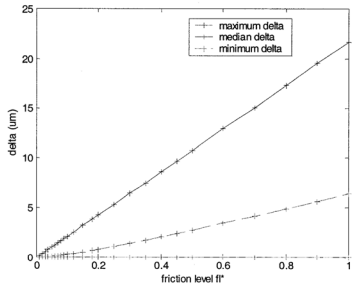

Fig.9 Delta versus friction level f_l* (simulation)

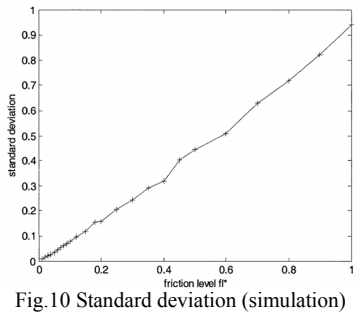

Fig.10 Standard deviation (simulation)

The following experiments are devised to verify the above simulation results, we put a wedge under the output arm and push the wedge towards the arm to increase the load side friction. We then measure the friction f_l and ca1culate the friction level f_l^* using equation (16). The resolution is then tested in the different friction levels. The histograms are plotted in Fig.11. The delta versus friction level is plotted in Fig.12. From these graphs, we can see that the resolution is degraded linearly to the friction level. The experimental results are consistent with the simulation. The standard deviation is plotted in Fig.13.

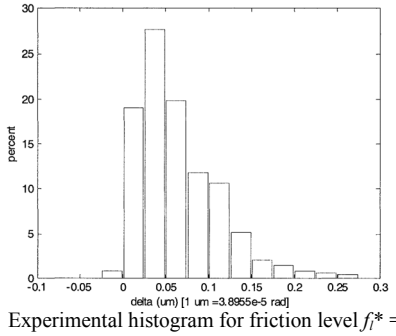

Fig.11 Experimental histogram for friction level f_l* =0.176

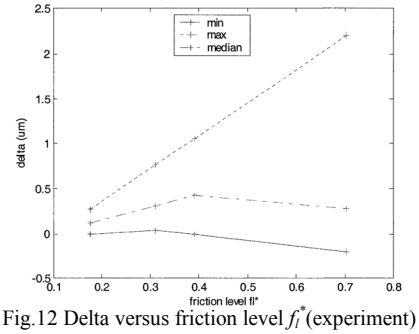

Fig.12 Delta versus friction level f_l^*(experiment)

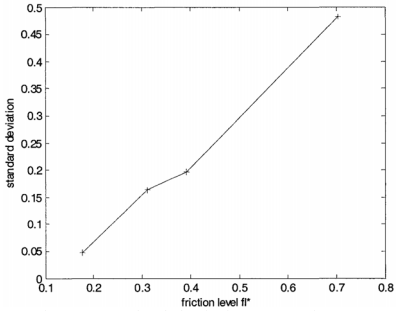

Fig.13 Standard deviation (experiment)

VI. CONCLUSION

The resolution of harmonic drives controller with friction in precision robotic system is comprehensive studied in this paper, This results demonstrate that the resolution of impulse controller can be increased by more than an order of magnitude over resolution of conventional control methods.

The simulation and experimental results shows that the load side friction level has a significant effect on the resolution in impulse control systems. The resolution gets worse proportionally as the load side friction level increases. It is therefore very important to account for load friction variations for impulse control to be effective.

The analysis will allow harmonic drives to be economically used in many new applications where high precision positioning capability is needed.

REFERENCES

[1] Stefani, R.T., Shahian, B., Savant, C.J., Hostetter, G.H. *Design of Feedback Control Systems,* Oxford University Press, 2002

[2] Marton, L. and Lantos, B. Modeling, identification, and compensation of stick–slip friction, *IEEE Transaction Industry Electronics*, 2007, 54(1):511–521

[3] Jatta, F., Legnani, G., and Visioli, A. Friction compensation in hybrid force/velocity control of industrial manipulators, *IEEE Transaction Industry Electronics*, 2006, 53(2):604–613.

[4] Khayati, K., Bigras, P., and Dessaint, L.-A. A multistage position/force control for constrained robotic systems with friction: joint-space decomposition, linearization, and multiobjective observer/controller synthesis using LMI formalism. *IEEE Transaction Industry Electronics*, 2006, 53(5):698–1712.

[5] Li G.-J. and Chen S-M., Study of a New Dynamic Model for Harmonic Drive in Precision Control System, *Journal of university of Electronic Science and Technology of China,* 2010, 39(5):742-746.